NON-LINEAR INSERTS FOR THE IOTA RING*

F.H. O'Shea†, R.B. Agustsson, and Y. Chen, RadiaBeam Technologies, LLC, Santa Monica, CA, USA
D.W. Martin, J.D. McNevin and P.-S. Chang, RadiaBeam Systems, LLC, Santa Monica, CA, USA

Abstract

We present here the complete non-linear insert for the IOTA ring at Fermilab. In particular, we will show the results for the magnetic measurements and a discussion of leak correction in the unusually shaped vacuum chamber. A test assembly of the insert has been successfully completed and the insert functions mechanically as designed.

INTRODUCTION

The Integrable Optics Test Accelerator (IOTA) at Fermilab [1] is a proof-of-principle experiment of the Integrable Optics principle [2]. The dynamic aperture of the 40 m circumference ring will be probed using a 150 MeV electron beam, which will later be replaced with a ~3 MeV proton beam that will experience significant non-linear space charge forces. RadiaBeam's contribution to the IOTA project is the design and construction of the non-linear insert (see Fig. 2). The development of the non-linear insert can be followed through a series of conference proceedings [3–5] and presentations [6–8].

NON-LINEAR INSERT STATUS

Assembly of the non-linear insert is complete, all of the parts have passed mechanical check for fit, and it has been shipped to Fermilab. After a number of corrective actions were taken, the vacuum chamber has failed a hermiticity check at the location of one of the electron beam welds between a vacuum pump port and the main vacuum chamber. Otherwise, the magnetic axis of the magnet modules have been measured, the current settings have been determined and all of the modules have been installed on the main strongback. Because of the very tight fit between the vacuum chamber and the magnets, installation of the vacuum chamber is a process of partial disassembly of the magnets, then chamber installation and then reassembly of the magnets. This process is to ensure that the magnets to not puncture the 0.010 inch thick chamber walls near the pole faces. The design of the both the chamber and the magnets incorporated this feature from the very beginning, so the process is straightforward.

A two-tier motion system allows adjustment of the entire strongback relative to the beam line using a push-pull screw system while the eighteen magnet modules are aligned relative to each other using a series of off-the-shelf optical stages with custom adaptors between them. The bottom pole faces are permanently fixed to a plate containing alignment monuments for measurement of the location of the magnetic axis and alignment. The insert is longitudinally symmetric

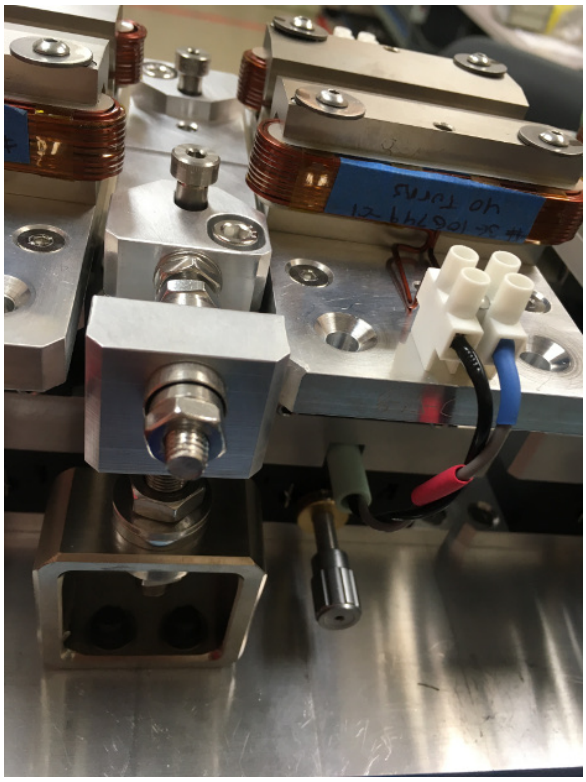

Figure 1: A vacuum chamber support stand is shown (center) in between two magnet modules. The conical alignment monuments for the magnet modules are seen to the front right.

to match the beam dynamics of the drift that it fills. Following this symmetry, there are nine different types of magnet module with each pair wired in series.

In half of the spaces between the magnets there are vacuum chamber support stands that are used to deform the vacuum chamber to clear the pole faces during assembly and operation (see Fig. 1). These stands have three axes of motion.

The aluminum vacuum chamber has five flanges installed, consisting of beam ports on either end that incorporate space for button-type beam position monitors, and three flanges on top for vacuum pumping. The vacuum chamber uses a large ante chamber to increase vacuum pumping speed at the small diameter (~8 mm) beam pipe.

MAGNETIC MEASUREMENTS

To comport with the theory, the strength of the magnet modules is designed to scale quadratically with longitudinal position in the drift that is filled with non-linear insert [2].

* Work supported by DOE under contract DE-SC0009531.
† oshea@radiabeam.com

ISBN 978-3-95450-182-3

Figure 2: The fully assembled IOTA insert.

Because of this, the apertures of the magnets in the nonlinear insert also scale quadratically. Before installation of the magnet modules, we performed two types of magnetic measurement on the different modules. The first was a gradient measurement to determine the correct current setting and the second was a vibrating wire measurement to find the magnetic axis of each module. When powered, the magnets are run through a standardization routine in which the current is run to +2 A, the maximum of the bi-polar power supplies to be used at Fermilab, then the current is slowly swept through the full current range (-2 A to +2 A) twice before approaching the operation point from -2 A. This procedure resulted in shifts of the magnetic axis smaller than we are capable of detecting.

To find the appropriate magnet current setting without performing a magnetization curve measurement for the iron, we measured the gradient (lowest harmonic) of one of each type of magnet module as a function of input current. We rely on the tight mechanical tolerances and the good harmonic content of the prototype magnets and do not measure the harmonic content of the magnets above quadrupole. The measured field gradient is very linear as a function of input current (see Fig. 3).

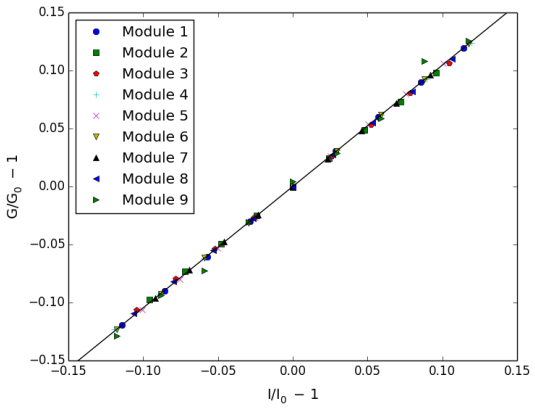

Figure 3: Plot of the normalized gradient deviation as a function of the normalized current distribution for one of each of the modules.

The vibrating wire system for magnet axis finding is a hybrid between the SLAC system [9] and the Paul Scherrer system [10] in which the transverse motion is automated but the yaw and pitch motion is not. The automation was necessary to repeatably measure the roll with sufficient precision to meet the magnet alignment requirements (see Fig. 4(bottom)). The axis finding routine works very near to the noise floor and occasional obviously erroneous measurements must be rejected (see Fig. 4(top)). In addition, there is significant steady-state background that must be subtracted from the signal, likely due to the magnetization of elements of the mechanical system.

ISBN 978-3-95450-182-3

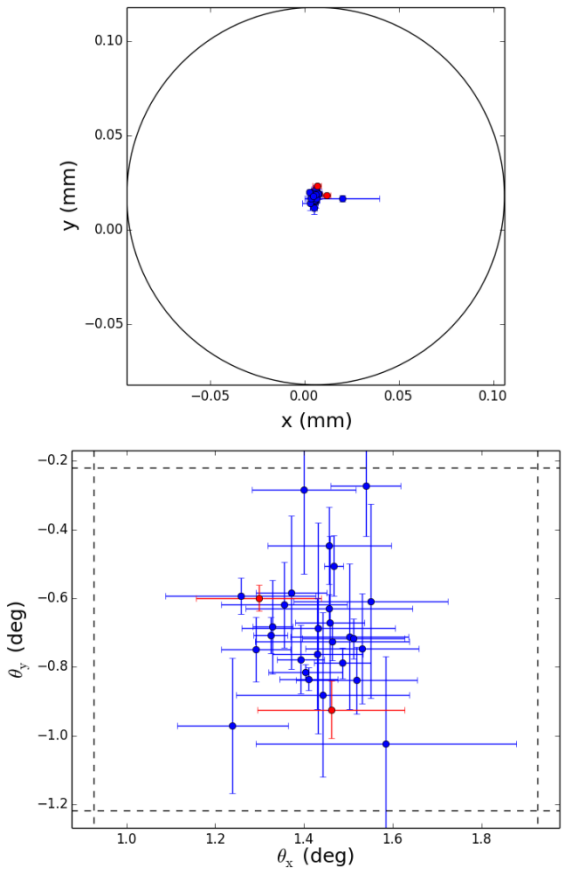

Figure 4: Measurement results for a typical module. (top) The repeated value of the magnetic axis as measured by the motor step counter is compared to the allowed deviation (black circle). There is an obvious outlier in the axis location. (bottom) The roll of the magnet calculated using the axis data, as compared to the allowed deviation (dashed lines). The two different roll calculations come from measuring where either B_x or B_y is zero. The differing mean values for θ_x and θ_y suggests that the two detectors are not normal to each other. The red points are those that were measured using the absolute arm.

VACUUM SYSTEM

We opted for a very complex vacuum chamber design because the magnet module apertures vary along the length of the insert and we want to maximize clear aperture. The chamber is manufactured in parts that are electron beam welded together. The main vacuum chamber is nine parts made of 2219 aluminum and there are also five flanges that use an explosion bonded transition from stainless steel to 6061 aluminum. The vacuum chamber was fabricated in three stages where parts would be made, welded and then modified before further welding to produce the final two meter long chamber.

While the vast majority of these welds worked (including all the welds on the prototype chamber), the weld of the center vacuum pumping port flange to the main chamber failed a hermiticity check in the 10^{-8} torr·liter/sec range. After consultation with the welders, we concluded that the leak was caused by poor joining of the 2219 aluminum of the main chamber to the 6061 aluminum of the pumping port. To attempt a fix on this weld, we cut the flange out, created a 6061-to-2219 adaptor that was TIG welded to the flange and attempted another electron beam weld. Unfortunately, this weld has also failed a hermiticity check. Because of the very local nature of the leak (in a different location from the previous one), our current working theory is that the tack weld (done in air) that held the flange to the vacuum chamber during electron beam welding (done in vacuum) created a pocket of oxidation that prevented the electron beam weld from creating a clean joint.

REFERENCES

[1] A. Valishev, S. Nagaitsev, V.V. Danilov, and D.N. Shatilov in *Proc. IPAC'12*, pp. 1371.

[2] V. Danilov and S. Nagaitsev, *Phy. Rev. ST Accel. and Beams*, vol. 13, p. 084002, 2010.

[3] F.H. O'Shea, *et al.* in *Proc. NAPAC'13*, pp. 922.

[4] F.H. O'Shea, *et al.* in *Proc. IPAC'15*, pp. 724.

[5] J.D. McNevin, R.B. Agustsson and F.H. O'Shea in *Proc. NAPAC'16*, pp. TUPOB39.

[6] F.H. O'Shea, "Design and Measurement of IOTA non-linear insert magnets," presented at 16^{th} Advanced Accelerator Concepts, San Jose, CA, USA, Jul. 2014, unpublished.

[7] F.H. O'Shea, "Non-linear Magnetic Field Inserts for the IOTA Ring," presented at 19^{th} International Magnetic Measurement Workshop, Hsinchu, Taiwan, Oct. 2015, unpublished.

[8] F.H. O'Shea, "Construction of the Non-linear Insert for the IOTA Ring," presented at 17^{th} Advanced Accelerator Concepts, National Harbor, MD, USA, Jul. 2016, unpublished.

[9] Z. Wolf, "A Vibrating Wire System For Quadrupole Fiducialization," SLAC, Palo Alto, CA, USA, Rep. LCLS-TN-05-11, May 2005.

[10] C. Wouters, M. Calvi, V. Vrankovic, S. Sidorov, and S. Sanfilippo, *IEEE Trans. Appl. Supercon.*, vol. 22, p. 9001404, 2012.

ISBN 978-3-95450-182-3